Ellipsometry and electron diffraction study of anodically formed Pd oxide layers

A. E. Bolzán, J. O. Zerbino, E. Macchi and A. J. Arvia

Instituto de Investigaciones Fisicoquímicas Teóricas y Aplicadas (INIFTA), Facultad de Ciencias Exactas, Universidad Nacional de La Plata, Sucursal 4, Casilla de Correo 16, (1900) La Plata (Argentina)

Abstract

Anodic Pd oxide films grown in 1 M H_2SO_4 and 1 M $HClO_4$ during the time τ ($15\ s \leqslant \tau \leqslant 9000\ s$) at the potential E_τ($1.90\ V \leqslant E_\tau \leqslant 2.06\ V$) have been investigated by ellipsometry and electron diffraction techniques. Ellipsometry confirms the duplex structure of the anodic Pd oxide films earlier concluded from electrochemical data. Electron diffraction reveals epitaxial growth of PdO on Pd at early stages. The film thickness fits a logarithmic growth rate equation for oxide layer thicknesses greater than 10–20 nm, depending on the solution composition.

1. Introduction

The electrochemistry of Pd oxides formed at high positive potentials was first considered about 70 years ago [1] and has been more thoroughly examined in recent years [2–4]. Particular attention has been paid to Pd oxide film formation and electroreduction [4], as well as to the composition and structure of those layers producing rough Pd surfaces [2, 3], but a number of questions still remain without convincing answers. This is the case, for instance, of the actual oxidation level of Pd at the anodic layer in relation to the kinetics and mechanism of Pd oxide growth at high positive potentials.

This work reports on ellipsometry and electron diffraction data of Pd oxide layers produced at constant potentials in acid solutions. From these data, the early stages of growth can be described as the epitaxial growth of PdO on Pd. A logarithmic rate equation for the anodic layer growth when the layer thickness exceeds about 10–20 nm, depending on the solution composition, has been obtained.

2. Experimental details

The experimental set-up for the ellipsometric measurements has been described in a previous publication [5]. The working electrode was a Pd disk(Johnson Matthey Chemical Co., spec. pure, 0.12 cm^2 geometric area) axially embedded in a cylindrical Teflon holder, which was mechanically polished with 0.3 μm–0.05 μm grit Al_2O_3–water suspensions to produce a mirror surface. Electrode potentials were measured against a reversible hydrogen electrode immersed in either aqueous 1 M H_2SO_4 or aqueous 1 M $HClO_4$ prepared from p.a. grade reagents and Milli-Q* water. Runs were made at 25 °C.

The values of Δ, the phase shift, and Ψ, the amplitude ratio, of the initial Pd surface were measured at 0.4 V. The Pd electrode was first cycled in the solution between 0.30 V and 1.50 V to obtain a reproducible voltammogram. Later, it was stepped to E_τ ($1.93\ V \leqslant E_\tau \leqslant 2.06\ V$) during a time τ ($15\ s \leqslant \tau \leqslant 9000\ s$) and then stepped to 1.6 V to measure Δ and Ψ. After the ellipsometric measurement the potential was reset to E_τ to continue the oxide film growth. Repetitive runs showed that the change from E_τ to 1.6 V had no effect on the oxide film growth. Values of Δ and Ψ at 1.6 V for different film thicknesses d were obtained at six wavelengths (405, 450, 492, 546, 580 and 671 nm). By assuming an isotropic and homogeneous film, the experimental data were fitted according to a modelling routine described elsewhere[6].

The electron diffractograms were obtained with a Siemens Elmiskop 101 electron microscope, furnished with a liquid N_2 anticontamination device and a cooling stage, at an acceleration potential of 100 kV. Double-condenser illumination conditions were applied with the first condenser lens fully energized, and a 20 μm aperture fitted to the second[7]. In this way, the influence of the second condenser's spherical aberration was kept to a minimum, and the irradiated regions of the specimens were restricted to very small surface areas ($\pm 1\ \mu m^2$). Calibration of the microscope column, to establish the diffraction constant, was accomplished by recording electron diffraction patterns of vacuum-deposited Au films. Specimen preparation was carried out by electropolishing small Pd disks using an LiCl–methanol solution in a Tenupol-III (Streuers) polishing device.

0040-6090/93/$6.00

TABLE 1. Optical constants of Pd at different wavelengths

λ (nm)	405	450	492	546	580	671
n	2.546	2.777	2.977	3.247	3.368	3.795
k	1.538	1.594	1.682	1.786	1.996	2.145

3. Results

The optical constants of Pd (n, the refractive index, and k, the absorption coefficient) at 0.40 V and different λ are in good agreement with data reported in the literature [8, 9] (Table 1).

The Δ *vs.* Ψ plots resulting from Pd oxide layers grown at $E_\tau = 2.03$ V in 1 M H_2SO_4 (Fig. 1) depend on λ. For $\lambda \leqslant 546$ nm as d increases the Δ *vs.* Ψ plot moves counterclockwise, whereas for $\lambda > 546$ *nm* the opposite behaviour is observed. As λ is changed from 546 nm upwards, the ellipsometric plots move circularly with d as expected for a non-absorbing film, whereas as λ is changed downwards those plots shift as expected for an absorbing film.

At $E_\tau = 1.90$ V, a slight variation in n with λ (Fig. 2(a)) is observed for a constant d value, but the magnitude of n depends on whether $d < 21$ nm or $d > 30$ nm. Pd oxide layers with thicknesses in the 10 nm $\leqslant d \leqslant$ 21 nm range appear to have a water content greater than that of those films with $d > 30$ nm. The n *vs.* λ (Fig. 2(b)) and the k *vs.* λ (Fig. 2(d)) plots obtained at $E_r = 2.03$ V exhibit the same trend in the dependence of these plots on d, but the overall effect is smaller than that found at $E_\tau = 1.90$ V. Seemingly, for $d > 30$ nm n increases with d as one would expect for an oxide film

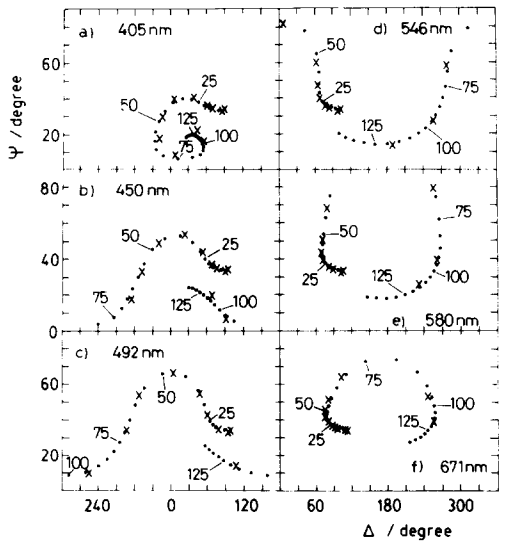

Fig. 1. Δ *vs.* Ψ plots measured at 1.6 V (×) after anodizing the electrode at 2.03 V in 1 M H_2SO_4 at different times. ·····, calculated using the fitted data. Film thicknesses in nanometres are indicated.

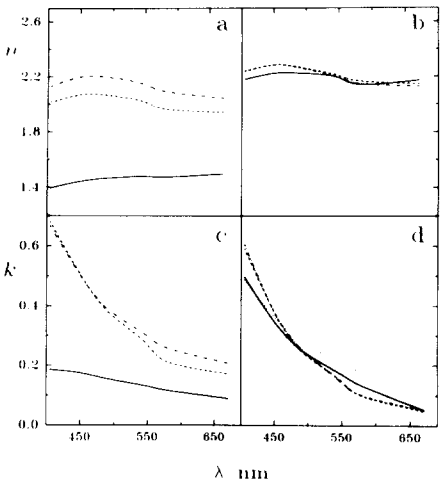

Fig. 2. n and k *vs.* λ plots at (a), (c) $E_\tau = 1.90$ V and (b), (d) $E_\tau = 2.03$ V for different oxide layer thickness values (1 M H_2SO_4): (a), (c) ——, 11 nm; ·····, 21 nm; – – –, 31 nm; – · · –, 42 nm; (b), (d) ——, 18 nm; ·····, 40 nm; , 92 nm; · · , 116 nm.

in which the water content decreases as d is increased. These features are also reflected in the k *vs.* λ plots (Fig. 2(c)). These plots reveal a continuously increasing absorption of Pd oxide films in the UV spectral region. This effect is much greater for $d < 21$ nm, and is enhanced for $d > 30$ nm. Between $\lambda = 671$ nm and $\lambda = 405$ nm a nearly tenfold increase in absorptivity is found when d is changed from 21 to 42 nm.

For both 1 M $HClO_4$ and 1 M H_2SO_4 the Pd oxide layer growth follows a logarithmic rate law in the 1.90 V $\leqslant E_\tau \leqslant$ 2.06 V range (Fig. 3). Only at the earlier stages of growth is a zero-order kinetics approached. These results agree with the structure of Pd oxide layers produced at E_τ values in this range. As concluded from

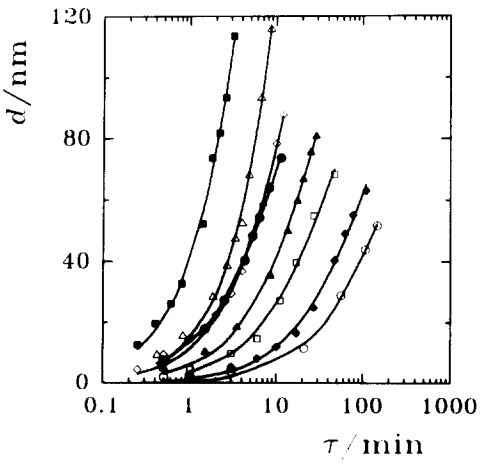

Fig. 3. Anodization time τ dependence of the oxide layer thickness d for 1 M H_2SO_4 (■, 2.06 V; △, 2.03 V; ◇, 2.00 V; ▲, 1.96 V; ◆, 1.93 V; ○, 1.90 V) and 1 M $HClO_4$ (□, 1.93 V; ●, 2.00 V). ——, calculated with the parameters assembled in Table 3.

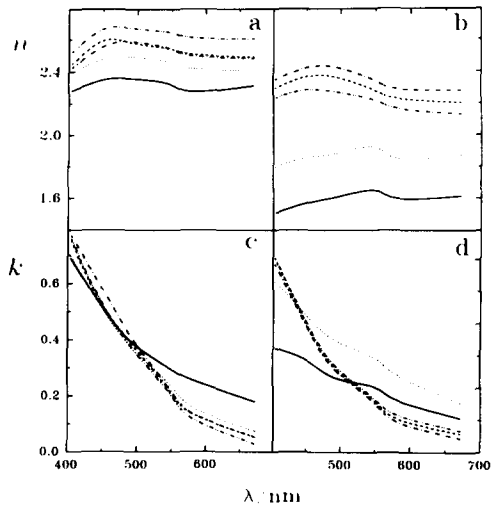

Fig. 4. n and k *vs.* λ plots at $E_\tau = 2.00$ V in (a), (c) 1 M H_2SO_4 and in (b), (d) 1 M $HClO_4$. (a), (c) ——, 9 nm; ·····, 20 nm; – · · –, 41 nm; – – –, 56 nm; – · –, 88 nm. (b), (d) ——, 20 nm; ·····, 29 nm; – · · –, 44 nm; – – –, 53 nm; – · –, 63 nm.

electrochemical data the Pd oxide layer structure consists of a thin inner and a relatively thicker outer oxide layer [4].

Ellipsometric data of Pd oxide films depend on the solution composition. In general, at constant λ and d, the values of n in 1 M H_2SO_4 are greater than those in 1 M $HClO_4$ (Fig. 4). The same trend can be observed for k at $\lambda < 400$ nm, although in this case the change in n with d is much smaller than that in k with d. Likewise, it appears that the influence of the inner Pd oxide layer ($d < 21$ nm) on the value of n is diminished in going from 1 M $HClO_4$ to 1 M H_2SO_4. Seemingly, the thickness of the inner Pd oxide layer and the water content of the Pd oxide layer in 1 M H_2SO_4 are lower than in 1 M $HClO_4$. These results are consistent with the influence of the water–anion interactions at the Pd oxide–solution interface, which in 1 M H_2SO_4 are stronger than in 1 M $HClO_4$ [10].

Diffraction patterns arising from Pd foils anodized at 2.06 V for 10 min clearly demonstrate the crystallographically related coexistence of Pd and PdO. From the indexing of the reflections (Fig. 5) it follows that the specimens exhibit a textured morphology with the [101] metal direction and the [010] oxide direction perpendicular to the foil surface (*i.e.* parallel to the electron beam direction). The epitactic character of the metal ⟶ oxide process is evidenced by the relative positions of the corresponding reflections in the pattern, which point to the following crystallographic relationships: (111) Pd ‖ (101) PdO and (200) Pd ‖ (002) PdO. Epitaxial growth of PdO on Pd has also been reported for surface reactions under vacuum conditions [11]. The single-crystal character of the two-dimensional electron diffraction pattern derived from such experiments indicates that the average lateral extension of the single-crystal metal grains should be at least 1 μm in diameter. Small, satellite reflections crystallographically related to and superimposed on the main diffraction pattern derive from the presence of smaller grains brought about by secondary nucleation. The crystallographic parameters derived from these experiments are reported in Table 2.

TABLE 2. Comparison of crystallographic parameters of Pd and PdO derived from electron diffraction data (d_{obs}) and tabulated data (d_{tab}) taken from ref. 18

Species	*hkl*	d_{obs} (nm)	d_{tab} (nm)
Pd	111	0.225	0.2667
	200	0.196	0.1945
PdO	101	0.263	0.2644
	002	0.269	0.2667

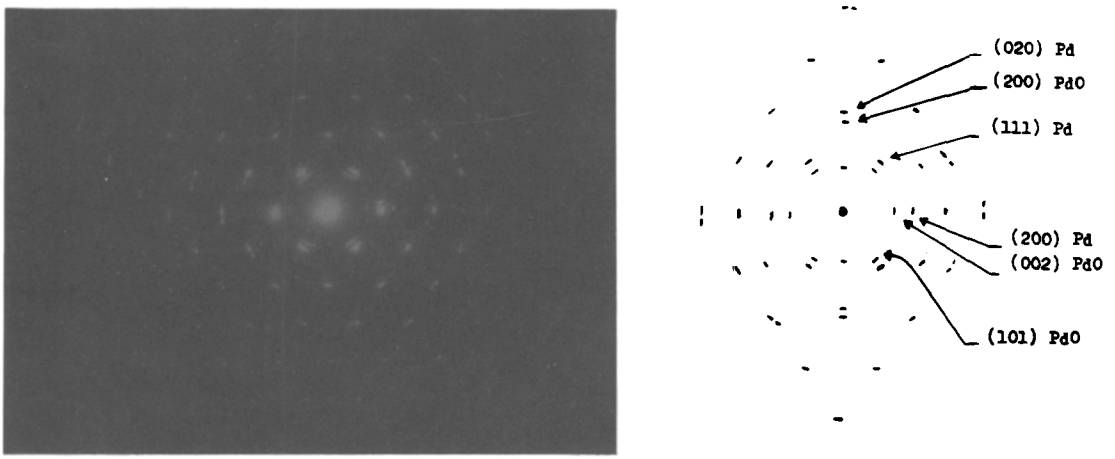

Fig. 5. Electron diffraction pattern of the PdO film grown at 2.06 V for 10 min in 1 M H_2SO_4.

4. Discussion

The Pd oxide layers formed at $E_\tau \geqslant 1.90$ V behave as light-absorbing films, the absorption coefficient increases toward the UV region, and the band gap of the oxide film should probably be greater than 3 eV. The absorptivity values found in the visible region suggest the presence of an appreciable concentration of defect states within the band gap of the oxide, which contribute to the electronic conductivity of the film. Therefore, the optical behaviour of Pd oxide films becomes largely similar to that found for Pt oxide films grown at nearly the same potential [13].

As seen in Fig. 4, for $d > 9$ nm in 1 M H_2SO_4 and for $d > 21$ nm in 1 M $HClO_4$, the value of n increases with d, *i.e.* with the anodization time. This fact suggests that the water content in the Pd oxide film probably diminishes as the average film thickness is increased. A similar effect is observed by either increasing the anodization potential or using 1 M H_2SO_4 instead of 1 M $HClO_4$. Hence, the composition of the Pd oxide films can be formally represented as $PdO \cdot xH_2O$, with $1 \leqslant x \leqslant 4$, where x depends on the solution composition.

According to electron diffraction data PdO and $PdO \cdot xH_2O$ present the same tetragonal structure, the a axis decreasing and the c axis increasing with the water content [14, 15]. Although the accuracy of the electron diffraction pattern does not allow a quantitative determination of the water content, the constants obtained for the Pd oxide layers anodically grown (Table 2) are consistent with the presence of residual water. Seemingly, Pd oxide layers can incorporate either O atoms or H_2O molecules without changing their crystallographic structure. As the PdO_2 is known to be less stable than PdO [16], it should be expected that the former species may decompose under the vacuum conditions used to perform the electron diffraction experiments.

The anodic Pd oxide film growth obeys a logarithmic rate law as would be expected for the growth of conducting oxides involving ion migration as the rate-determining step. Assuming that the free energy of activation increases linearly with the average Pd oxide layer thickness, the rate equation in terms of d can be written as follows [12]:

$$dd/dt = A \exp[-(\Delta G^{\ddagger}_{0,e} + bd)/RT] \qquad (1)$$

where b denotes the rate of change of $\Delta G^{\ddagger}_{0,e}$ with the film thickness, $\Delta G^{\ddagger}_{0,e}$ is the activation free energy of the electrochemical process at $d = 0$, A is a pre-exponential factor, d is the average Pd oxide layer thickness, and R and T have their usual meanings.

For an electrochemical reaction $\Delta G^{\ddagger}_{0,e} = \Delta G^{\ddagger}_{0,c} + \alpha z F \eta_a$, where $\Delta G^{\ddagger}_{0,c}$ is the chemical contribution to $\Delta G^{\ddagger}_{0,e}$, α is the transfer coefficient assisting the reaction in the anodic direction, z is the number of electrons entering the reaction, and η_a is the anodic overvoltage defined as $\eta_a = E_\tau - E_0$. E_τ is the anodization potential and E_0 is a reference potential related to the Pd oxide electrode. Then, the integration of eqn. (1) with the boundary condition $d = 0$ for $t = 0$ gives

$$d = (RT/b) \ln\{(b/RT)\, A' t \exp[\alpha z F(E_\tau - E_0)/RT] + 1\} \qquad (2)$$

where A' is a constant containing the potential-independent activation free energy terms. For the different Pd oxide films, after applying the Levenberg–Marquardt minimization procedure, eqn. (2) accounts for the experimental data (Fig. 3) with the fitting parameters assembled in Table 3.

TABLE 3. Fitting parameters for Pd oxide layer growth at different anodization potentials

E_τ (V)	b (J nm^{-1})	$A \times 10^4$ (nm min^{-1})	αz	E_0 (V)
1 M H_2SO_4				
1.90	61	5.4	1.72	1.79
1.93	55	3.4	1.61	1.80
1.96	41	2.6	1.62	1.80
2.00	26	1.3	1.55	1.81
2.03	15	4.6	1.14	1.80
2.06	10	4.0	1.14	1.80
1 M $HClO_4$				
1.93	54	4.2	1.72	1.79
2.00	5	4.6	1.14	1.80

According to data shown in Table 3, the value of b decreases nearly linearly with the applied potential. This means that the activation energy for the oxide layer growth decreases as E_τ is set more positive, *i.e.* the electrical conductance of the film becomes larger as the value of E_τ is increased. The pre-exponential factor A fluctuates around $3.3 \pm 2.0 \times 10^{-4}$ nm min^{-1} in the potential range of the experiments. Similarly, the value of E_0, which remains practically constant (1.80 ± 0.01 V), corresponds to the potential region where the O_2 evolution reaction begins to take place on Pd in acid solutions, and it can be associated with the formation of highly oxidized Pd intermediates, and may play an important role in both the oxide layer formation and the oxygen evolution reaction itself. Finally, the product αz decreases with E_τ. If one assumes $z = 2$ for the global electron transfer reaction, this means that α decreases from 0.86 to 0.57 as E_τ is increased from 1.90 V to 2.06 V. It should be noted that the same change in α has been recently reported for the oxygen evolution reaction on oxide-coated noble metal electrodes in acid solutions [17]. In these cases, the change in α has been assigned to a potential-dependent composition of the noble metal oxide coating. These results

confirm recent electrochemical data on the influence of anions on anodic Pd oxide layer formation [10].

In conclusion, a consistent explanation and a good agreement with electrochemical, ellipsometric and electron diffraction data concerning the behaviour of anodic Pd oxide layers on Pd in acid solutions has been reached.

Acknowledgments

This work was financially supported by the Consejo Nacional de Investigaciones Científicas y Técnicas (CONICET), the Comisión de Investigaciones Científicas de la Provincia de Buenos Aires (CIC) and Fundación Antorchas. A.E.B. and J.O.Z. are members of the Research Center of CIC.

References

1 F. Jirsa, *Z. Phys. Chem.*, *113* (1924) 241.
2 L. D. Burke and M. B. C. Roche, *J. Electroanal. Chem.*, *186* (1985) 139.
3 V. Chausse, P. Regull and L. Victorí, *J. Electroanal. Chem.*, *238* (1987) 115.
4 A. E. Bolzan and A. J. Arvia, *J. Electroanal. Chem.*, *322* (1992) 247.
5 J. O. Zerbino, C. De Pauli, D. Posadas and A. J. Arvia, *J. Electroanal. Chem.*, *330* (1992) 675.
6 J. O. Zerbino, W. J. Plieth and G. Kossmehl, *J. Electroanal. Chem.*, *260* (1989) 361.
7 E. Macchi, *Makromol. Chem.*, *191* (1990) 2217.
8 M. A. Ordal, L. L. Long, R. J. Bell, S. E. Bell, R. R. Bell, R. W. Alexander and C. A. Ward, *Appl. Opt.*, *22* (1983) 1099.
9 J. T. Lue, H. W. Chen and S. I. Lew, *Phys. Rev.*, *34* (1986) 5438.
10 A. E. Bolzán and A. J. Arvia, *J. Electroanal. Chem.*, *354* (1993) 243.
11 H. Q. Ye, X. G. Ning and D. J. Smith, *Surf. Sci.*, *250* (1991) 90.
12 M. A. Genshaw, in E. Gileadi (ed.), *Electrosorption*, Plenum, New York, 1967, Chap. 4.
13 S. Gottesfeld, G. Maia, J. B. Floriano, G. Tremiliosi-Filho, E. E. Ticianelli and E. R. González, *J. Electrochem. Soc.*, *138* (1991) 3219.
14 O. Glemser and G. Peuschel, *Z. Anorg. Allg. Chem.*, *281* (1955) 44.
15 J. Waser, *Acta Crystallogr*, *6* (1953) 661.
16 K. S. Kim, A. F. Gossmann and N. Winograd, *Anal. Chem.*, *46* (1974) 197.
17 A. E. Bolzán and A. J. Arvia, *Proc. 42nd ISE Meet., Montreux, 1991* ISE, Montreux, 1991.
18 *Powder Diffraction File*, ASTM, Philadelphia, PA, Cards 5-0683, 6-0517, 9-256.